Adsorption of Gas Molecules on HfSSe Janus Monolayer

Ghufran Falah Ibrahim Witwit[1*], Dr. Shurooq Sabah Abed Al-Abbas[2]

Abstract

The density functional theory (DFT) method have already been used to study the electronic, optical and the adsorption properties of (CO, CO_2, NO, NO_2, SO_2) gas molecules on HfSSe (Se and S) monolayer. Initially, the properties of pristine HfSSe monolayer are calculated. The band gap of HfSSe (Se and S) monolayer is estimated to be 0.626eV which authorize the semiconducting behavior. The results show that the adsorption of gases occurs at different sites on the studied monolayer. However, every the adsorption energies are negatives and the adsorption of gas molecules on this monolayer undergoes physisorption interaction, thus they can be used to detecting gas molecules. The refractive indices of HfSSe-S monolayer are larger than that in HfSSe-Se monolayer, and reach to 2.50 and 2.31 of CO_2 and SO_2gases, approximately. On the opposite, the reflection peaks of the monolayer occur in the UV region range which agrees with the absorption coefficient. Besides, the maximum value of reflectivity in the adsorbed systems does not exceed 60%.

Key Words: Adsorption, HfSSe Janus Monolayer, Electronic Structure, Optical Properties.

DOI Number: 10.14704/nq.2022.20.1.NQ22069 **NeuroQuantology 2022; 20(1):150-161**

Introduction

Attributable to its band gap referred to the fact, layer that is atomic structure thick, unusual density of states, and mechanical strength, two-dimensional (2D) transition metal di-chalcogenides (TMDCs) have attracted a lot of attention in the field of electronics and optoelectronics in recent years (Wang et al. 2012). Several recent experiments reveal that they could be incredibly intriguing materials beyond 2D graphene with a tolerable band gap for a range of applications, electronic (Johari and Shenoy 2012), optoelectronic (Mak and Shan 2016), thermoelectric (Qin et al. 2018), sensing of gas (Perkins et al. 2013), splitting of water (Voiry, Yang, and Chhowalla 2016), and piezoelectric applications (Mleczko et al. 2017). These TMDCs, which have the generic formula MXY (where M=Mo, W, Hf, Zr, Pt, etc. and X, Y=S, Se, and Te), are layered materials with extremely crippled Van-der Waal interlayer contact, with one transition metal wedged between two layers by two chalcogen atoms layers. Lately, Ang-Yu Lu and colleagues (Ang-Yu Lu et al) (Lu et al. 2017). The top layer S atoms in monolayer MoS_2 were totally replaced by Se atoms, resulting in Janus monolayer MoSSe with in-plane inverting symmetry is broken, as is out-of-plane mirrored similarity. Giving cues from the world of Synthesis in the lab (Lu et al. 2017) (Sun et al. 2017). Various research on the electrical, optical, mechanical, thermoelectric, photocatylatic, sensing of gas, and mechanical characteristics of Janus monolayer MoSSe have already been carried out (Guan, Ni, and Hu 2018).

Corresponding author: Ghufran Falah Ibrahim Witwit

Address: [1*]Department of Physics, College of Education for Pure Sciences, University of Babylon, Iraq; [2]Ministry of Education, Babylon Education Directorate.

[1*]E-mail: Ghufran.falah.pure302@student.uobabylon.edu.iq

Relevant conflicts of interest/financial disclosures: The authors declare that the research was conducted in the absence of any commercial or financial relationships that could be construed as a potential conflict of interest.

Received: 17 November 2021 **Accepted:** 24 December 2021

Computational Methods

DFT techniques, which were run using the CASTEP program with leveraging the PBE and ultrasoft pseudopotentials and exchange-correlation energy functionals, were used to examine the electronic and optical characteristics of monolayer HFXY (XY= S, Se) (Clark Stewart et al. 2005; Perdew, Burke, and Ernzerhof 1996).

A 8×8×1 k-mesh Monkhorst-Pack grid is used to evaluate the Brillouin zones. The optical characteristics were computed with 30×30×1 Monkhorst pack k-mesh, while the density of state computations were done with 24×24×1. This k-point level is critical for displaying a material's optical spectra, particularly the unreal component of the dielectric function. All calculations are done on a plane wave basis with a kinetic energy cut-off of 470 eV. All atoms in these Janus structures are totally relaxing, in conjunction with convergence criterion of for atoms are subjected to a total amount of energy and force., approximately. In the Z-direction10^{-6} eV and 0.01 eV/Å, a vacuum gap of 30 Å was employed to avoid contact between the consecutive monolayer. Nonetheless, the characteristics of light are questioned by the density functional perturbation theory with an energy range between 0 and 25 eV. These characteristics include the absorption coefficient α(ω), the energy loss function L(ω), imaginary (Im(ε(ω)) and real (Re(ε(ω)) parts of dielectric function ε(ω), refraction index n(ω), the reflectivity R(ω), where ω denoted the frequency of incident photons (Abed Al-Abbas, Muhsin, and Jappor 2019).

Adsorption Energy

A detailed investigation is carried out for adsorption of gas molecules at different websites utilizing the adsorption finder module to locate the places of reduced energy absorption of gas molecules adsorbates for the analysis of structural, electrical, and optical characteristics. The adsorption energy (E_{ad}) can be calculated according to (Liang et al. 2017),

$$E_{ad} = E_{tot} - (E_{Hfsse} + E_{gas}) \qquad (3.1)$$

Where E_{Hfsse} is the energy of monolayer (Se and S), E_{gas} is the energy of isolated gas molecules, and E_{tot} is the total energy of the system (Gas + monolayer). This is how this definition works, a value that is negative of E_{ad} indicates that the adsorption is energizing and exergonic favorable. Alternatively, positive adsorption the term "energy" connotes the polar opposite of the circumstance.

Table 1. The calculated adsorption energy (E_{ad}), the bond length between atoms in gas molecules (d) Å, at the gas molecules (NO, CO_2, CO, SO_2, and NO_2) and HfSSe (Se and S) monolayer

Gas molecules	Bond length(d) Å	E_{ad}(ev)
CO	CO-Se=3.632 CO-Hf=5.880 CO-S=5.342	CO-Se=-0.10354 CO-S=-0.10292
CO_2	CO_2-Se=4.458 CO_2-Hf=5.637 CO_2-S=5.512	CO_2-Se=-0.24137 CO2-S=-0.24236
NO	NO-Se=5.562 NO-Hf=5.562 NO-S=5.321	NO-Se=-0.26926 NO-S=-0.26926
NO_2	NO_2-Se=4.397 NO_2-Hf=5.645 NO_2-S=5.469	NO_2-Se=-1.46403 NO_2-S=-1.46403
SO_2	SO_2-Se=4.576 SO_2-Hf=5.926 SO_2-S=5.899	SO_2-Se=-1.97503 SO_2-S=-1.88768

To start with, adsorption energy is an indicator of impulse analysis. The more adsorption energy there is, the greater reliable the system under investigation is. Obviously, The adsorption energy plays a crucial role on material behavior features, as an instance physisorption or chemisorption. Furthermore, Us findings suggest all adsorption values are equal minus, implying that exergonic character of adsorption gas molecules is energetically beneficial. In this project, We investigate the adsorption of a number of typical polluting gas molecules, CO, CO_2, NO, SO_2 and NO_2 which are of great importance for industrial and environmental, on HfSSe (Se and S) monolayer based on DFT (Abed Al- Abbas, Muhsin, and Jappor 2018).

Electronic Properties of Adsorbed Molecules on Monolayer

The most advantageous arrangements of CO adsorbed on HfSSe on Se and S monolayer are shown in Fig. (1), During relaxation, certain atoms in this monolayer deform to some amount and travel exterior the plane. The bond length between (Hf–CO) of HfSSe monolayer are 5.880 Å and (Se-CO) are 3.632 Å and (S-CO) are 5.342 Å, respectively. Furthermore, because the massive adsorption distance and a minor charge transfer indicates C (Se-S) is physically adsorbed on monolayer via vdW interactions (J. Zhang et al. 2019). After adsorption, the band gaps of the adsorbed systems in CO HfSSe on Se (0.618 ev) and S (0.617 eV) display a little alteration as shown in Fig. (2). The total and partial densities of states (DOS and PDOS) of the adsorption systems are computed and displayed in Fig. (3) (a) and (b) to further demonstrate the interactions of the CO molecule on the various monolayer systems. It is found that the DOS of the

CO on monolayer during adsorption, there is a little shift, and the contribution of the CO electronic levels to the overall DOS is between (1.3-2)eV in the VBs and around (-3-4.2) eV in CBs, which is a long way from the Fermi level. This behavior is in the same way as adsorption of CO on phosphorene (Schedin et al. 2007), stanene (Luo et al. 2016), ZnO with graphene-like properties (Niu et al. 2019), and germanene (X. Zhang et al. 2017), and further confirming the weak interaction of CO molecule on monolayer system. Fig. (4) shows that the most stable configuration of CO_2 adsorbed on HfSSe are found from our result that the bond lengths between Hf-CO_2 of (5.637) Å. which essentially decreases as the number of electrons in the elements increases are similar to the adsorption of CO on HFXY monolayer. After adsorption the results of the band gaps of the adsorbed systems in HfSSe, Se (0.628 eV) and HfSSe, S (0.627 eV) show a slight change as shown in Fig. (5). Clearly, in this situation, the energy gap is expanded by a very modest amount of HfSSe, Se monolayer whereas the band gap of HfSSe, S monolayer is decreases under the effect of adsorption of CO_2. Kumar and Roy describe single layer stanane as having a similar behavior (Kumar and Roy 2019). Fig. (6). When gas molecules are adsorbed on a monolayer, the DOS in the valence and conduction bands of the molecules adsorbed on the monolayer is considerably changed. Gas molecules have a significant role in the electronic states of a molecular monolayer system. The conduction band, namely the area between 3 and 10ev, makes the biggest contribution. The adsorption structure of adsorbed NO on HfSSe of Se and S monolayer are shown in Fig. (7). The adsorption of different gas molecules on the electronic characteristics of monolayer HfSSe of Se and S monolayer were evaluated using the band structures of molecule-monolayer systems. When compared to a virgin monolayer HfSSe of Se and S in Fig. (8), there is no energy gap due to the interference of the valence beam with the conduction beam at the Fermi level for HfSSe of Se and S monolayer and this means that it is conductive. Fig. (9) displays the PDOS and TDOS of NO molecule interacts with the surface of HFXY after NO molecule adsorbed. The TDOS of the NO-HFXY near the Fermi level, the system displays a notable shift as well as a strong orbital hybridization. We can observe that when the NO is adsorbed on, the states over Femi energy vanish owing to the fixation of the N atom on the S atoms, which is comparable to the prior study (Ma et al. 2016). Fig. (10) shows top and side views of the adsorbed molecule NO_2 on the HfSSe of Se and S monolayer. Figure (11) shows the electronic properties of adsorbed NO_2 gas molecules on monolayer. Compared with the band structure before adsorption that presented, it is noted that after the adsorption of the NO_2 gas molecules, band gap varying is (0.628 and 0.639) eV for HfSSe of Se and S monolayer. In order to confirm the mechanics of the NO_2 adsorption interaction, the DOS and the PDOS of monolayer and molecules system are displayed in Fig. (12). Fig. (13) show the top and side views of the adsorbed molecule SO_2 on the HfSSe of Se and S monolayer, This also suggests that the desorption of SO_2 from HfSSe by UV irradiation would face more challenges (Tamalampudi et al. 2014), or an electrical field (Late et al. 2012). The band gaps of the adsorbed systems in HfSSe of Se is no energy gap due to the interference of the valence beam with the conduction beam at the Fermi level and this means that it is conductive and the band gap in HfSSe of S is (0.025 eV) show a prodigious change as evidenced by Fig. (14). The density of states (DOS) near the Fermi level appears to be mixed, for example there is a peak in –15 eV; and the DOS changes. Figure (15) shows that these mixed states are caused by SO_2 adsorption.

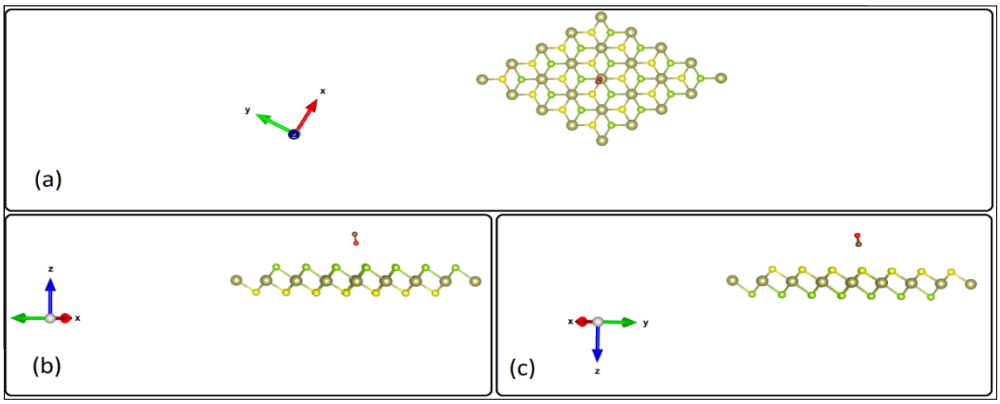

Fig. 1. (a) Top view of the adsorbed molecule CO on the HfSSe (b) side view Se and (c) side view S monolayer

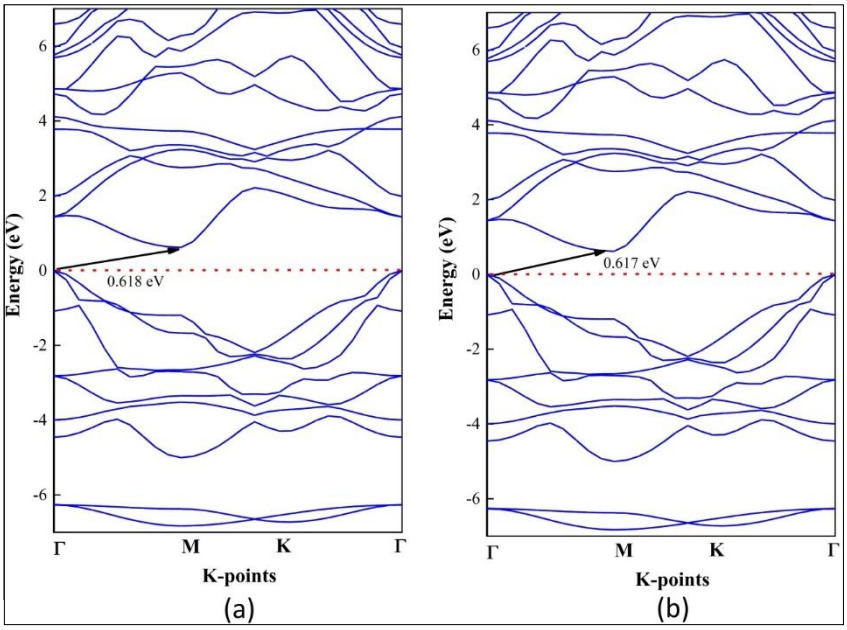

Fig. 2. Band Structures of HfSSe (a) Se and (b) S monolayer after the adsorption of CO gas

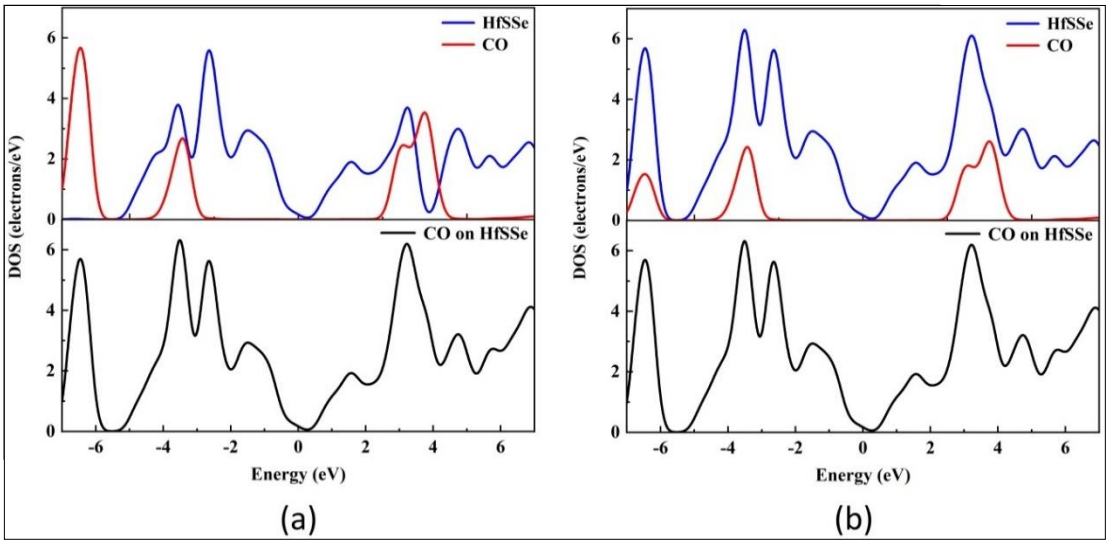

Fig. 3. DOS of HfSSe (a) Se and (b) S monolayer after the adsorption of CO gas

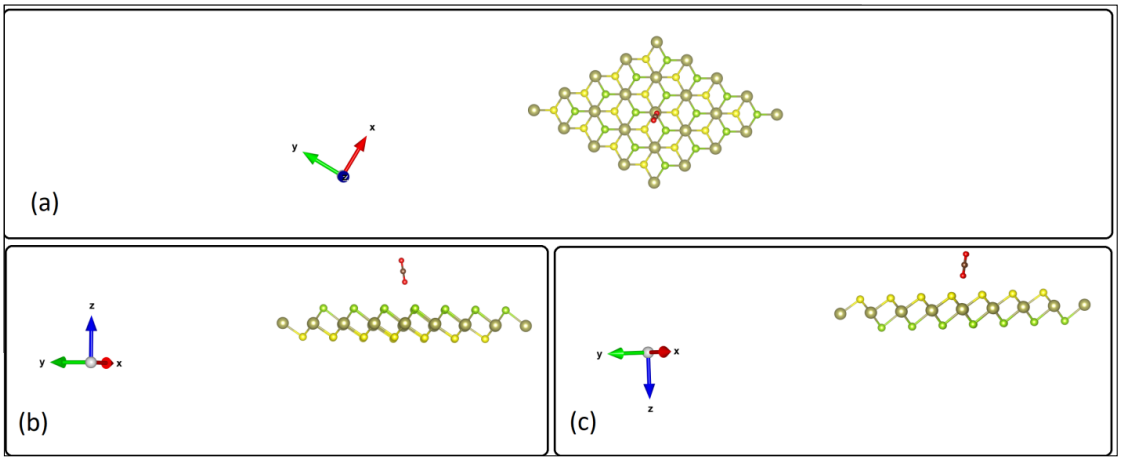

Fig. 4. (a)Top view of the adsorbed molecule CO_2 on the HfSSe (b) side view Se (c) side view S monolayer

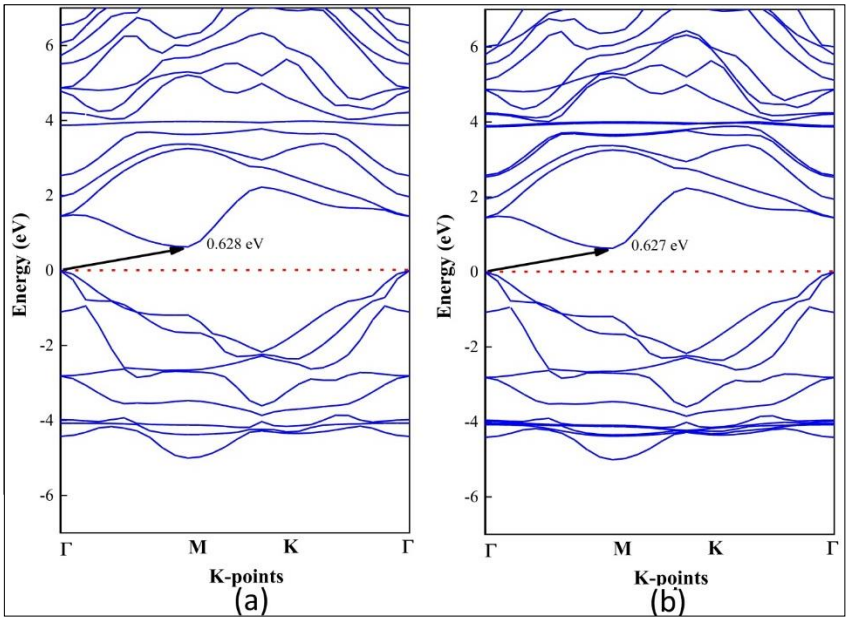

Fig. 5. Band structures on HfSSe of (a) Se and (b) S monolayer after the adsorption of CO_2 gas

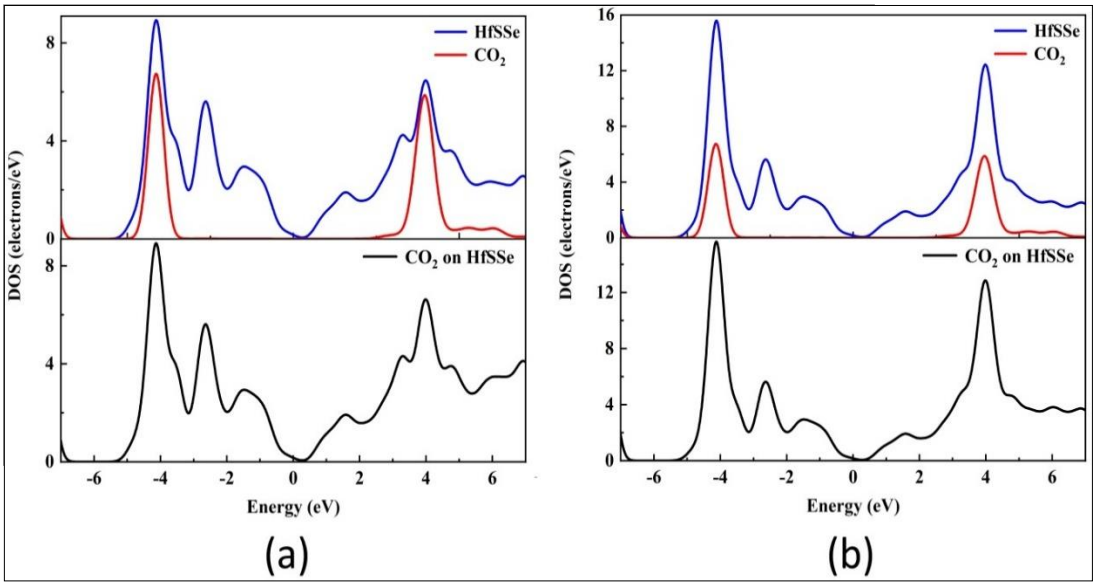

Fig. 6. DOS of HfSSe of Se and S monolayer after the adsorption of CO_2 gas

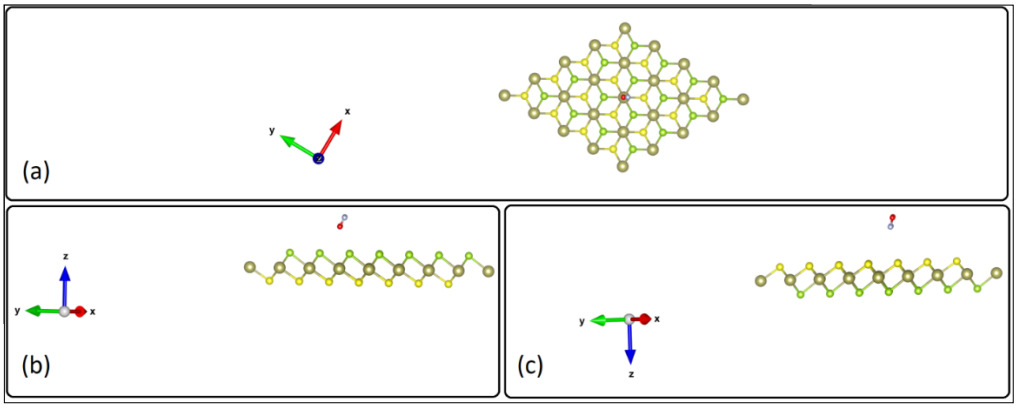

Fig. 7. (a) Top view of the adsorbed molecule NO on the HfSSe (b) side view Se and (c) side view S monolayer

*e*ISSN 1303-5150

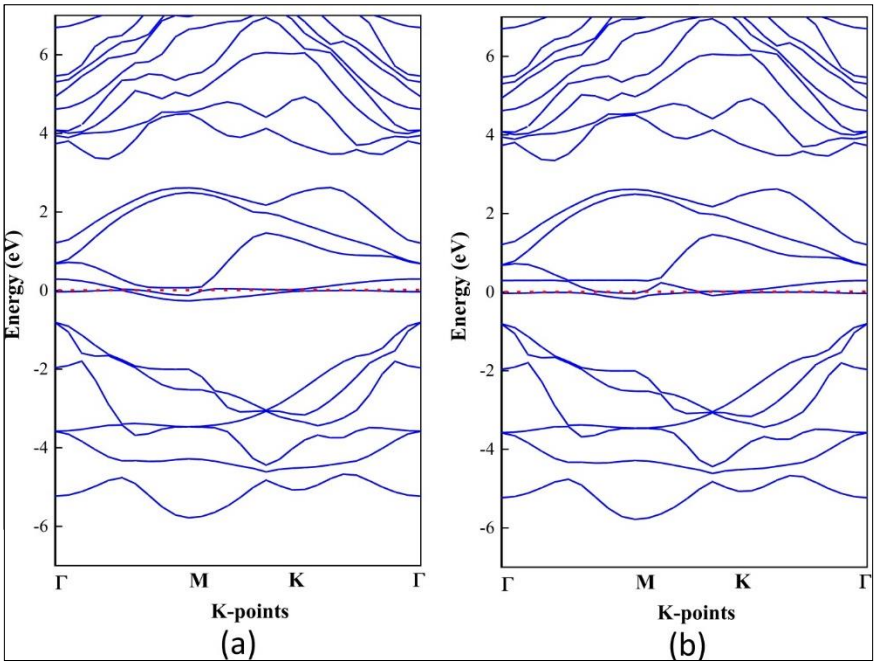

Fig. 8. Band structures of HfSSe (a) Se (b) S monolayer after the adsorption of NO gas

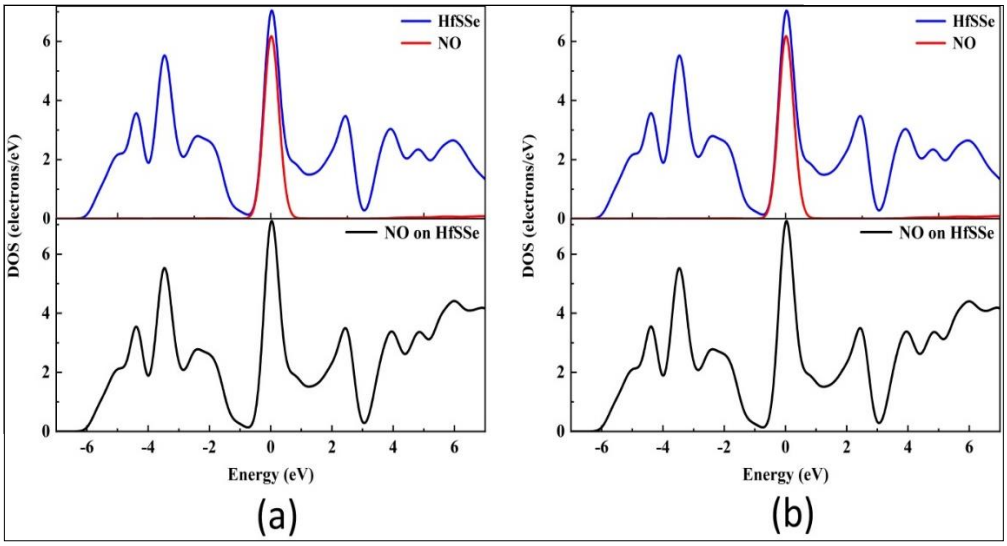

Fig. 9. PDOS and TDOS of HfSSe (a) Se and (b) S monolayer after the adsorption of NO gas

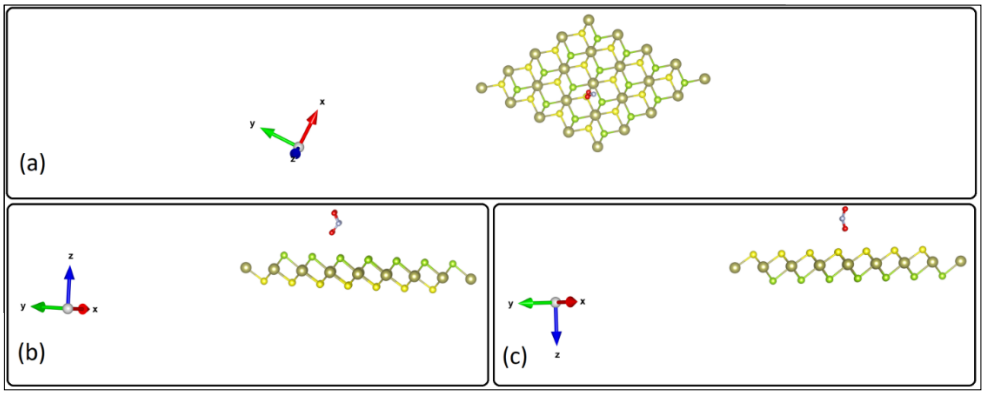

Fig. 10. (a) Top view of the adsorbed molecule NO_2 on the HfSSe (b) side view Se (c) side view S monolayer

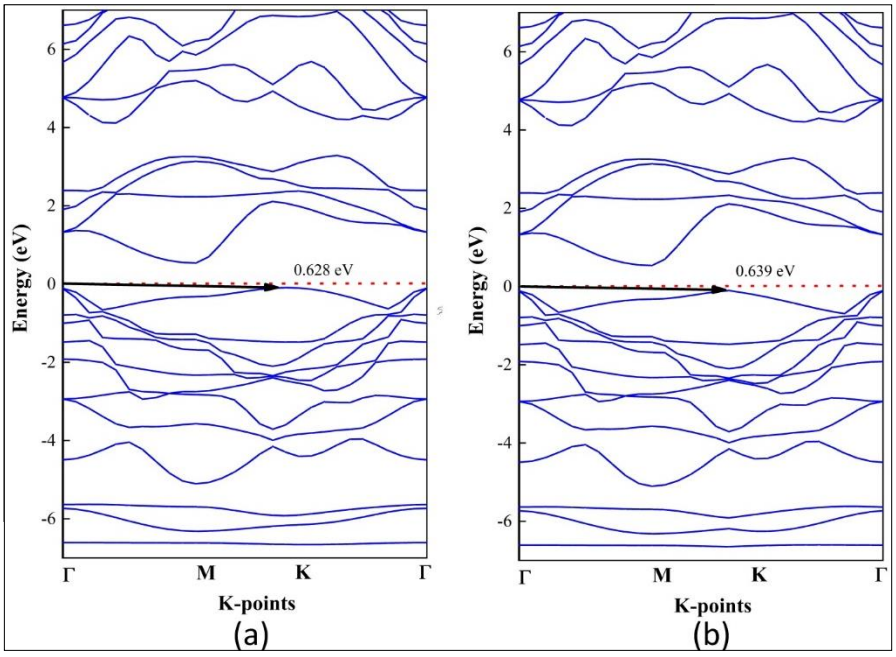

Fig. 11. Band structures of HfSSe (a) Se and (b) S monolayer after the adsorption of NO_2 gas

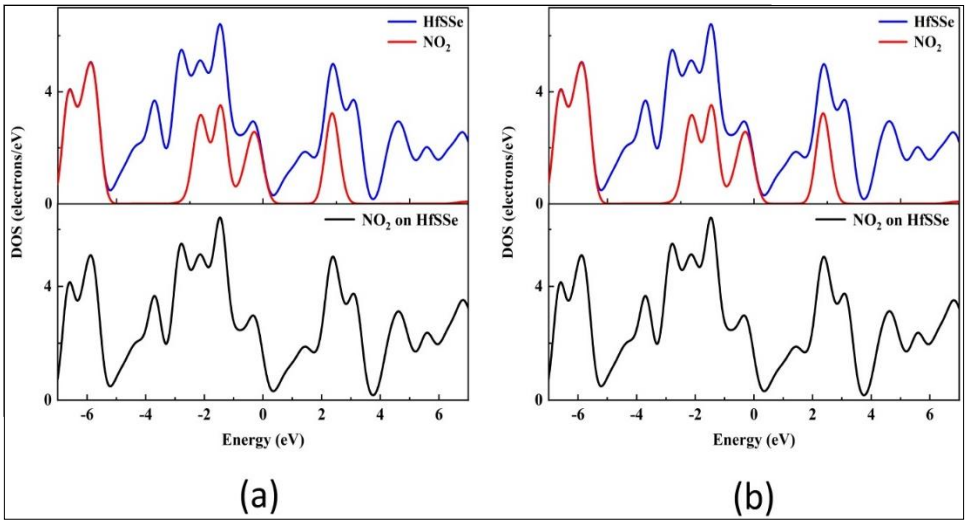

Fig. 12. DOS of HfSSe (a) Se and (b) S monolayer after the adsorption of NO_2 gas

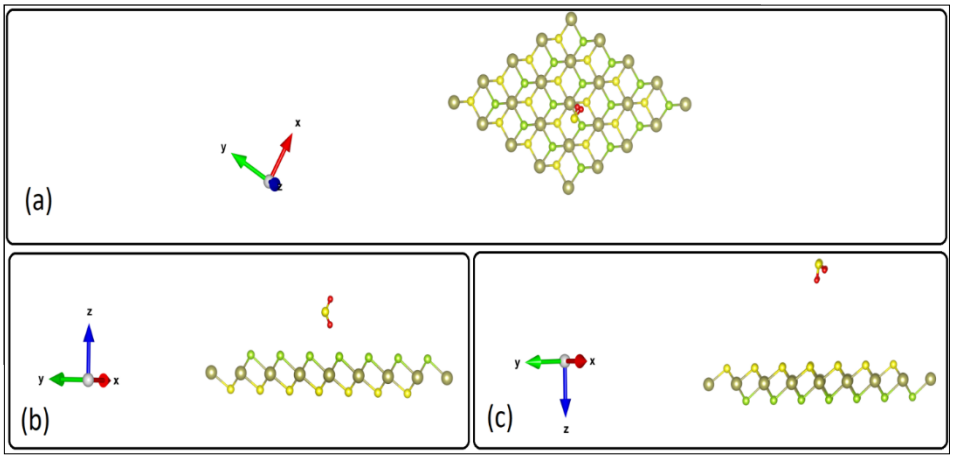

Fig. 13. (a) Top view of the adsorbed molecule SO_2 on the HfSSe (b) side view Se and (c) side view S monolayer

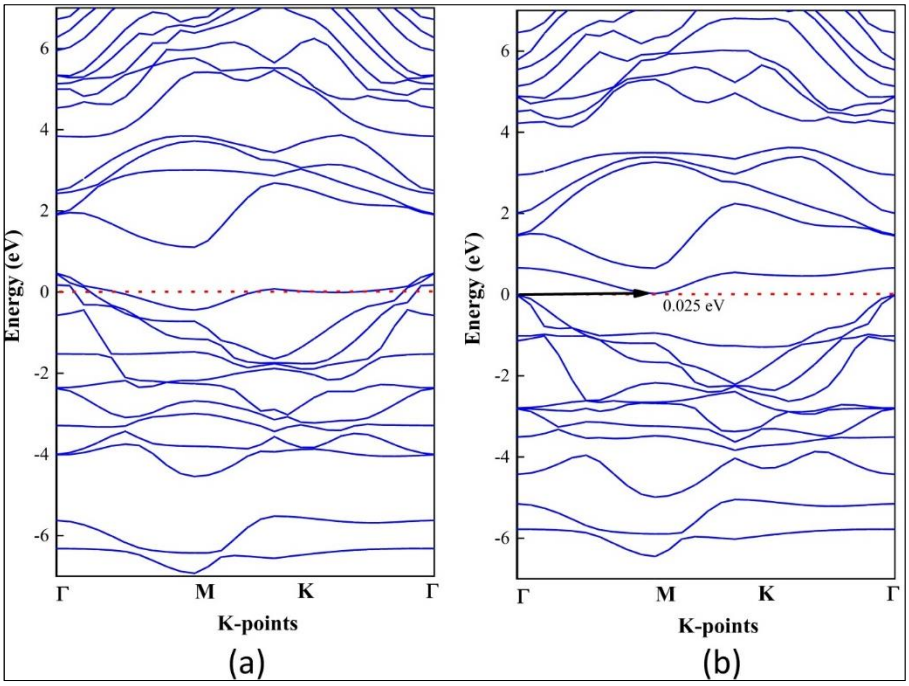

Fig. 14. The calculated band structures of HfSSe (a) Se (b) S monolayer after the adsorption of SO_2 gas

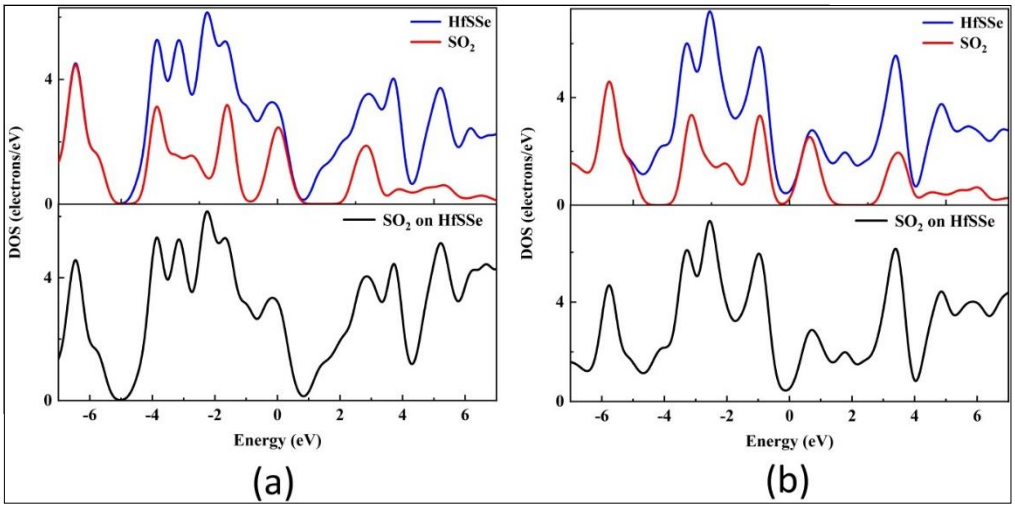

Fig. 15. DOS of HfSSe (a) Se and (b) S monolayer after the adsorption of SO_2 gas

Optical Properties of Adsorbed Molecules on Monolayer

The optical characteristics of HfSSe of Se and S monolayer owing to the adsorption of the prior gas molecules will be investigated next. We'll concentrate on the effect of adsorption on this monolayer in this section (Abdulameer, Abed Al-Abbas, and Jappor 2021). Up a certain level of energy to 25 eV, the optical characteristics of adsorbed HfSSe of Se and S monolayer are calculated.

The reflectivity curves of molecules adsorbed on HfSSe of Se and S monolayer are illustrated in Figs. (16). It is clear that the maximum reflectivity of this monolayer when the adsorption of gas molecules is dependent on the type of gas. As can be observed, the static reflectivity with the highest value is 60% for CO2 adsorbed on HfSSe of S monolayer and the most tiny static reflectivity is 16% for NO2 adsorbed on HfSSe of S monolayer.

Figs. (17) displays the graphs of absorption coefficients of molecules that are being adsorbed on HfSSe of Se and S monolayer. the value of CO_2/HfSSe of S monolayer maximum height absorption is the most significant, whose worth is 3.01×10^4 cm^{-1} is situated at 8.99 eV, Then there's the absorption peak of CO_2/HfSSe of Se monolayer (2.39×10^4 cm^{-1} at 9 eV) and then the absorption peaks CO/HfSSe of Se

monolayer (1.69×10^{4} cm^{-1} at 11.10 eV).

The refractive indices of monolayer as a function of photon energy are represented in Figs. (18) from which we determine the dynamic refractive index of monolayer. Adsorbed systems' static refractive indices almost similar between Se and S, except for SO_2 molecule adsorbed of HfSSe-Se monolayer, whose value is 2.36 of HfSSe-Se is alowest to 1.66 of HfSSe -S. In instance, The real dielectric constant and the refractive index graphs are very similar, When these two curves behave in the same way is nearly same, with just minor variations in values.

Figs. (19,20) display the dielectric function of gas molecules adsorbed on a surface as a function of photon energy on HfSSe of Se and S monolayer. In this section, the real (Re) and imaginary (Im) parts of dielectric function are calculated using polarization light perpendicular to the plane of monolayer surface.

When compared to a pristine monolayer, the genuine static dielectric functions of adsorbed systems drop after adsorption adsorbed CO_2 on HfSSe of S monolayer, which is the most valuable (5.6). Alternatively, adsorbed SO_2 molecule on HfSSe of S monolayer has the smallest number (2.1), which is equivalent to the reflectivity tends to result of the gas CO_2 molecule as we will show later. Figs. (21) shows the optical conductivity as a function of photon energy of HfSSe (S, Se) monolayer after the adsorption of gas molecules. The optical conductivity are ranging between 1.89×10^{15} sec^{-1} for SO_2/HfSSe-Se monolayer and 8.97×10^{15} sec^{-1} for CO_2/HfSSe-S monolayer. Figs. (22) shows the energy loss function as a function of the photon energy adsorbed on the molecules on HfSSe of Se and S monolayer When compared to the clean monolayer peak, gas molecules result in lesser peaks, excluding adsorbed CO_2 on HfSSe-S monolayer that Having a strong peak that is equivalent to 2.91 at 15.2 eV and adsorbed NO_2 on HfSSe-S monolayer.

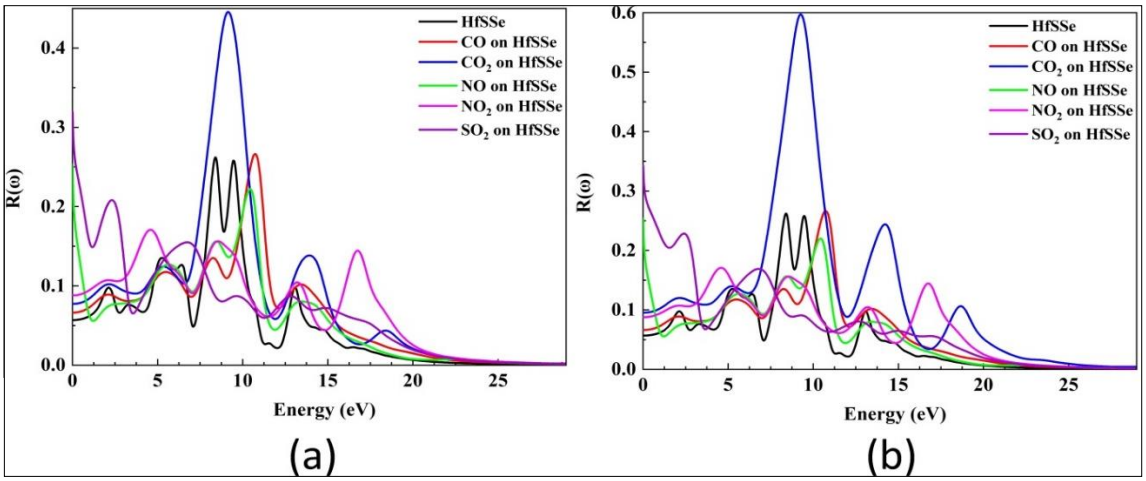

Fig. 16. The reflectivity as a function of energy of HfSSe: (a) Se and (b) S monolayer after the adsorption of NO, CO_2, CO, SO_2 and NO_2 molecules

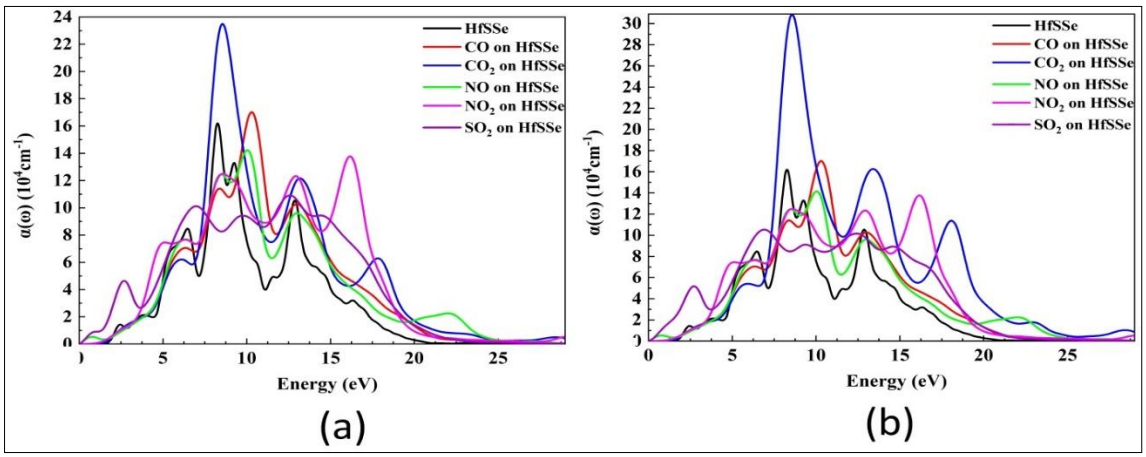

Fig. 17. The absorption coefficient as a function of photon energy of HfSSe:(a) Se and (b) S monolayer after the adsorption of NO, CO_2, CO, SO_2 and NO_2 molecules

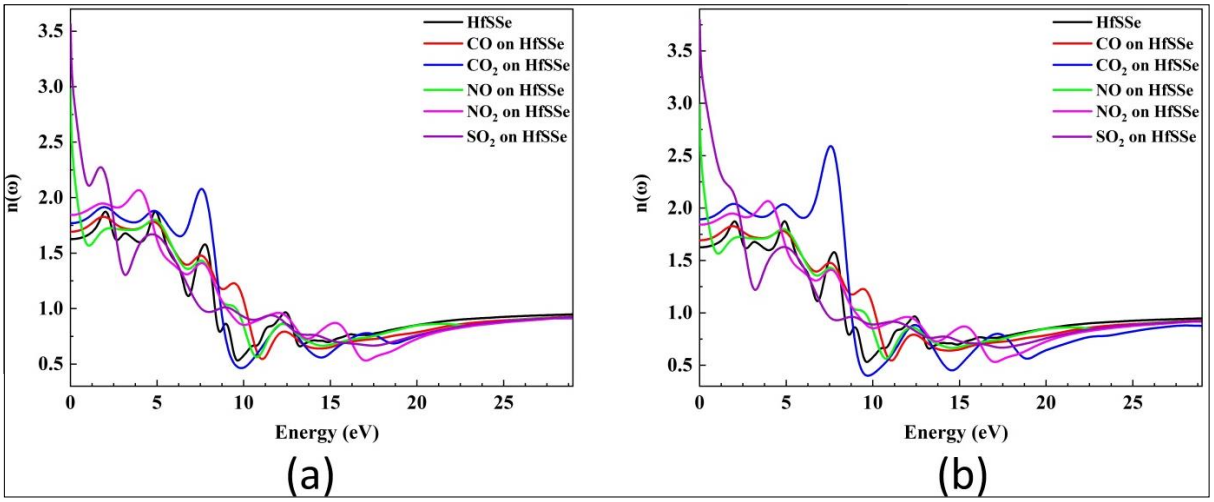

Fig. 18. The refractive index as a function of energy of HfSSe:(a) Se and (b) S monolayer after the adsorption of NO, CO_2, CO, SO_2 and NO_2 molecules

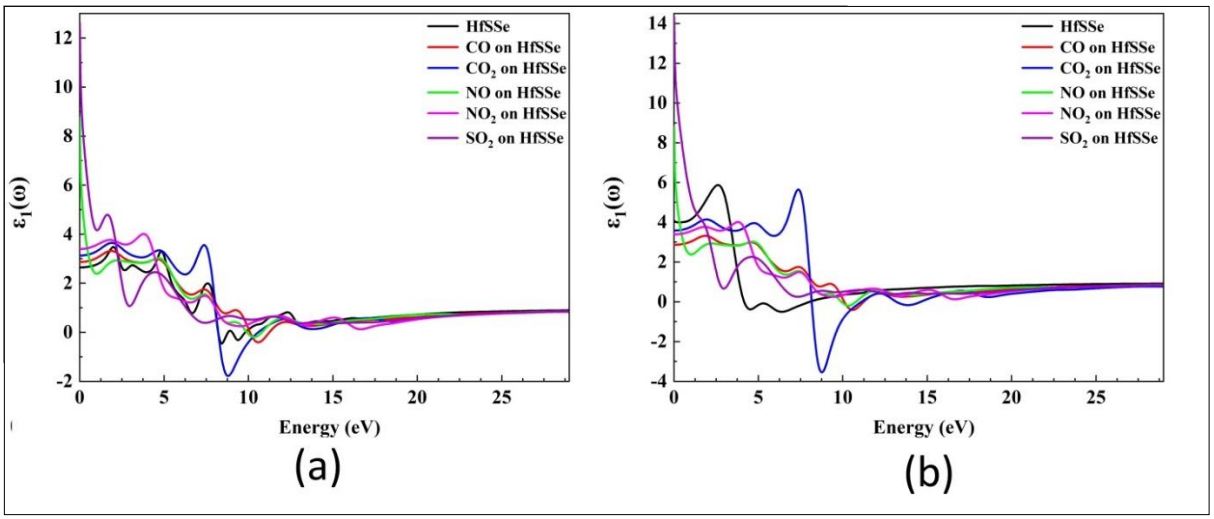

Fig. 19. Dielectric function Real as a function of photon energy of HfSSe: (a) Se and (b) S monolayer after adsorption of NO, CO_2, CO, SO_2 and NO_2 molecules

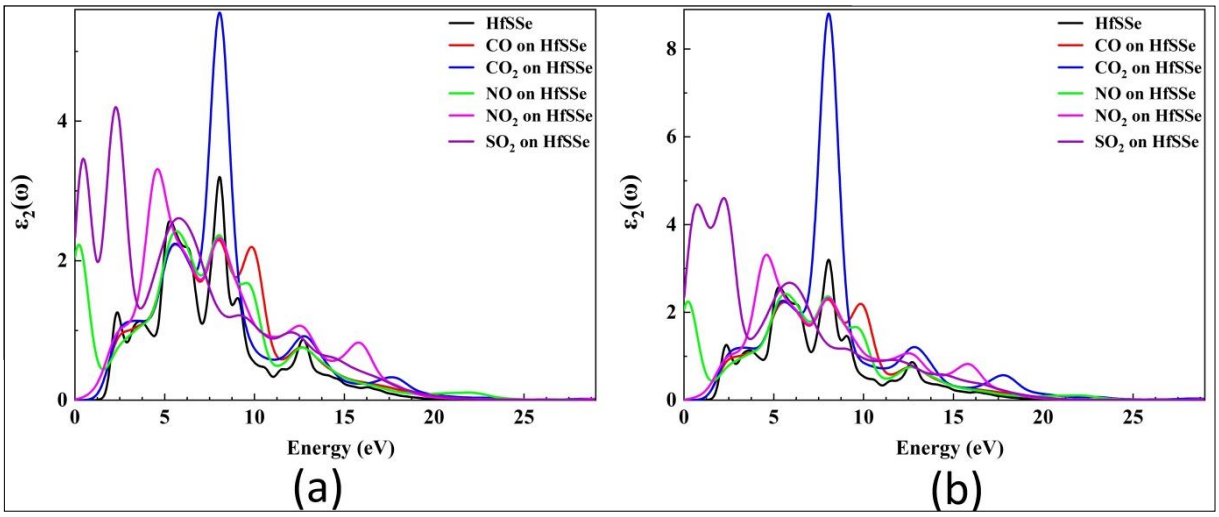

Fig. 20. Dielectric function Imaginary as a function of photon energy of HfSSe :(a) Se and (b) S monolayer after adsorption of NO, CO_2, CO,NO_2 and SO_2 molecules

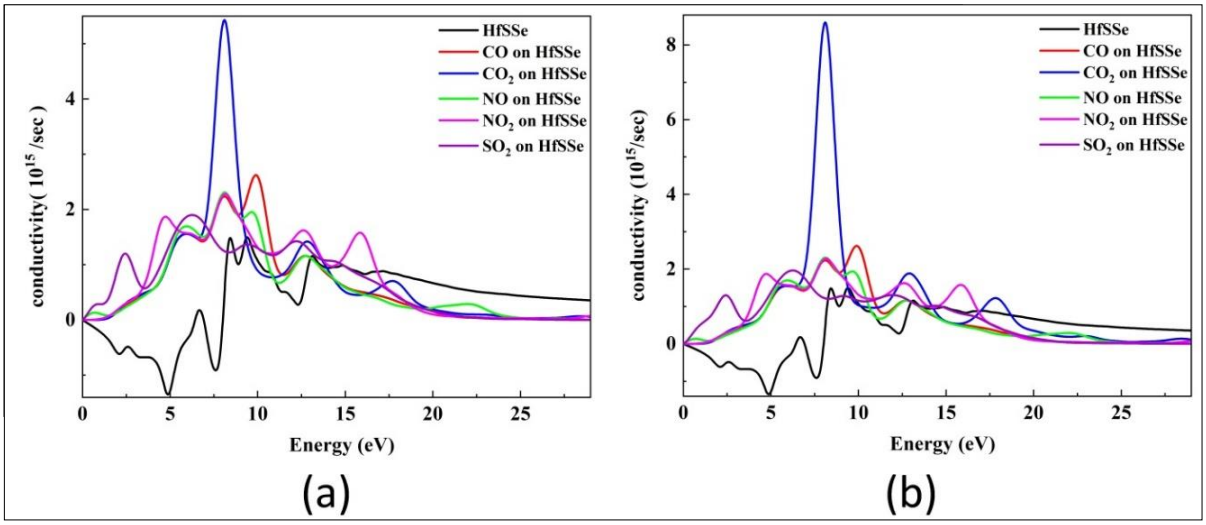

Fig. 21. The optical conductivity as a function of photon energy of HfSSe:(a) Se and(b) S monolayer after the adsorption of NO, CO_2, CO, SO_2 and NO_2 molecules

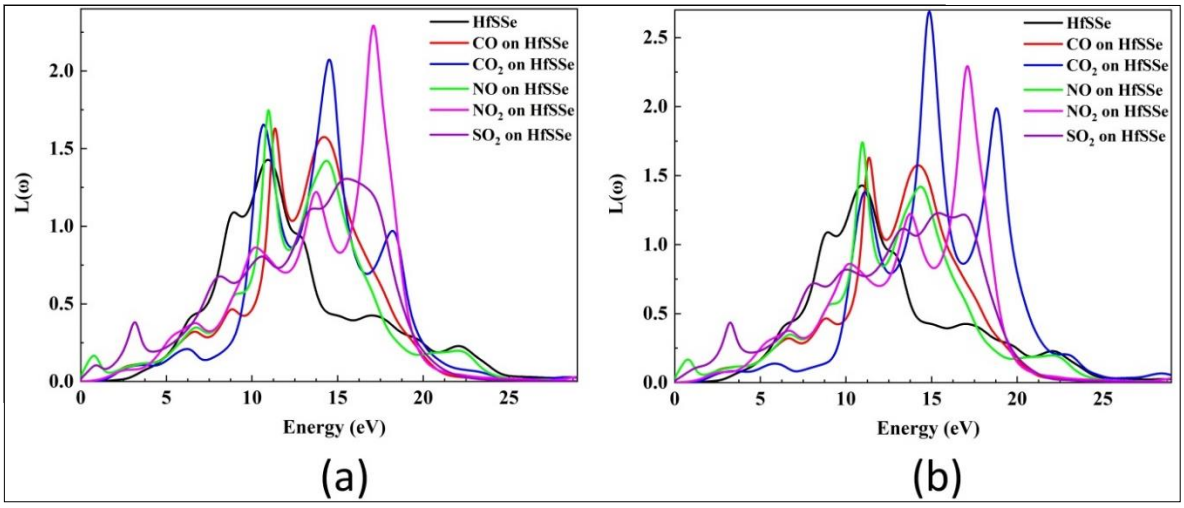

Fig. 22. The loss function as a function of energy of HfSSe:(a) Se and (b) S monolayer after the adsorption of NO, CO_2,CO,SO_2 and NO_2 molecules

References

Abdulameer MJ, Abed Al-Abbas SS, Jappor HR. Tuning optical and electronic properties of 2D ZnI2/CdS heterostructure by biaxial strains for optical nanodevices: A first-principles study. *Journal of Applied Physics* 2021: 129(22). https://doi.org/10.1063/5.0054365

Al-Abbas SSA, Muhsin MK, Jappor HR. Tunable optical and electronic properties of gallium telluride monolayer for photovoltaic absorbers and ultraviolet detectors. *Chemical Physics Letters* 2018; 713: 46-51. https://doi.org/10.1016/J.CPLETT.2018.10.020

Al-Abbas SSA, Muhsin MK, Jappor HR. Retracted: Two-dimensional GaTe monolayer as a potential gas sensor for SO2 and NO2 with discriminate optical properties. *Superlattices and Microstructures* 2019: 135. https://doi.org/10.1016/j.spmi.2019.106245

Clark SJ, Segall MD, Pickard CJ, Hasnip PJ, Probert MI, Refson K, Payne MC. First principles methods using CASTEP. *Zeitschrift für kristallographie-crystalline materials* 2005; 220(5-6): 567-570. https://doi.org/10.1524/zkri.220.5.567.65075

Guan Z, Ni S, Hu S. Tunable electronic and optical properties of monolayer and multilayer Janus MoSSe as a photocatalyst for solar water splitting: a first-principles study. *The Journal of Physical Chemistry C* 2018; 122(11): 6209-6216.

Johari P, Shenoy VB. Tuning the electronic properties of semiconducting transition metal dichalcogenides by applying mechanical strains. *ACS nano* 2012; 6(6), 5449-5456.

Kumar V, Roy DR. Single-layer stanane as potential gas sensor for NO2, SO2, CO2 and NH3 under DFT investigation. *Physica E: Low-dimensional Systems and Nanostructures* 2019; 110: 100-106. https://doi.org/10.1016/J.PHYSE.2019.02.001

Late DJ, Liu B, Matte HR, Rao CNR, Dravid VP. Rapid characterization of ultrathin layers of chalcogenides on SiO2/Si substrates. *Advanced Functional Materials* 2012; 22(9): 1894-1905. https://doi.org/10.1002/adfm.201102913.

Liang XY, Ding N, Ng SP, Wu CM L. Adsorption of gas molecules on Ga-doped graphene and effect of applied electric field: A DFT study. *Applied Surface Science* 2017; 411: 11-17.

https://doi.org/10.1016/J.APSUSC.2017.03.178

Lu Y, Ke C, Fu M, Lin W, Zhang C, Chen T, Wu Y. Magnetic modification of GaSe monolayer by absorption of single Fe atom. *RSC advances* 2017; 7(8): 4285-4290. https://doi.org/10.1039/C6RA27309B.

Luo H, Cao Y, Zhou J, Feng J, Cao J, Guo H. Adsorption of NO_2, NH_3 on monolayer MoS2 doped with Al, Si, and P: a first-principles study. *Chemical Physics Letters* 2016; 643: 27-33. https://doi.org/10.1016/j.cplett.2015.10.077

Ma D, Wang Q, Li T, He C, Ma B, Tang, Y, Yang Z. Repairing sulfur vacancies in the MoS_2 monolayer by using CO, NO and NO_2 molecules. *Journal of Materials Chemistry C* 2016; 4(29): 7093-7101. https://doi.org/10.1039/C6TC01746K.

Mak KF, Shan J. Photonics and optoelectronics of 2D semiconductor transition metal dichalcogenides. *Nature Photonics* 2016; 10(4): 216-226.

Mleczko MJ, Zhang C, Lee HR, Kuo HH, Magyari-Köpe B, Moore RG, Pop E. $HfSe_2$ and $ZrSe_2$: Two-dimensional semiconductors with native high-κ oxides. *Science advances* 2017: 3(8).

Niu F, Cai M, Pang J, Li X, Yang D, Zhang G. Gas molecular adsorption effects on the electronic and optical properties of monolayer SnP_3. *Vacuum* 2019: 168. https://doi.org/10.1016/J.VACUUM.2019.108823

Perdew JP, Burke K, Ernzerhof M. Generalized gradient approximation made simple. *Physical review letters* 1996; 77(18): 3865-3868. https://doi.org/10.1103/PhysRevLett.77.3865

Perkins FK, Friedman AL, Cobas E, Campbell PM, Jernigan GG, Jonker BT. Chemical vapor sensing with monolayer MoS_2. *Nano letters* 2013; 13(2): 668-673.

Qin D, Yan P, Ding G, Ge X, Song H, Gao G. Monolayer PdSe2: A promising two-dimensional thermoelectric material. *Scientific reports* 2018; 8(1): 1-8.

Schedin F, Geim AK, Morozov SV, Hill EW, Blake P, Katsnelson MI, Novoselov KS. Detection of individual gas molecules adsorbed on graphene. *Nature materials* 2007; 6(9): 652-655. https://doi.org/10.1038/nmat1967.

Sun G, Zhao P, Zhang W, Li H, He C. Adsorption of gas molecules on armchair AlN nanoribbons with a dangling bond defect by using density functional theory. *Materials Chemistry and Physics* 2017; 186: 305-311. https://doi.org/10.1016/J.MATCHEMPHYS.2016.10.058

Tamalampudi SR, Lu YY, Kumar UR, Sankar R, Liao CD, Cheng CH, Chen YT. High performance and bendable few-layered InSe photodetectors with broad spectral response. *Nano letters* 2014; 14(5): 2800-2806. https://doi.org/10.1021/nl500817g

Voiry D, Yang J, Chhowalla M. Recent strategies for improving the catalytic activity of 2D TMD nanosheets toward the hydrogen evolution reaction. *Advanced materials* 2016; 28(29): 6197-6206.

Wang QH, Kalantar-Zadeh K, Kis A, Coleman JN, Strano MS. Electronics and optoelectronics of two-dimensional transition metal dichalcogenides. Nature nanotechnology, 2012; 7(11): 699-712.

Zhang J, Yang G, Tian J, Wang Z, Tang Y, Ma D. Effect of atom adsorption on the electronic, magnetic, and optical properties of the GeP monolayer: A first-principle study. *Applied Surface Science* 2019; 475: 863-872. https://doi.org/10.1016/J.APSUSC.2019.01.046

Zhang X, Wang S, Wan G, Zhang Y, Huang M, Yi L. Transient reflectivity measurement of photocarrier dynamics in GaSe thin films. *Applied Physics B* 2017; 123(3): 1-7. https://doi.org/10.1007/s00340-017-6677-z